Journal of Materials Chemistry C

Accepted Manuscript

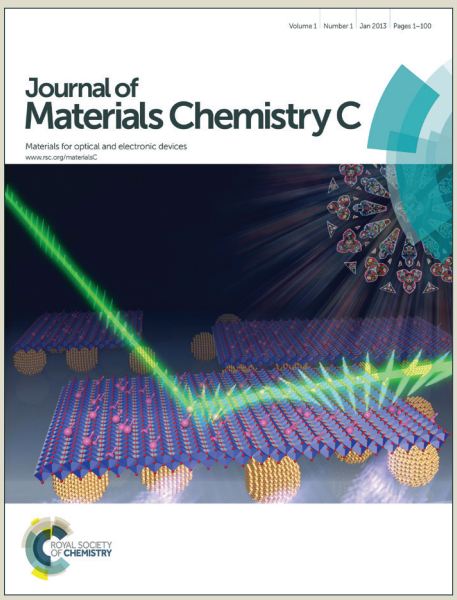

This is an *Accepted Manuscript*, which has been through the Royal Society of Chemistry peer review process and has been accepted for publication.

Accepted Manuscripts are published online shortly after acceptance, before technical editing, formatting and proof reading. Using this free service, authors can make their results available to the community, in citable form, before we publish the edited article. We will replace this *Accepted Manuscript* with the edited and formatted *Advance Article* as soon as it is available.

You can find more information about *Accepted Manuscripts* in the Information for Authors.

Please note that technical editing may introduce minor changes to the text and/or graphics, which may alter content. The journal's standard Terms & Conditions and the Ethical guidelines still apply. In no event shall the Royal Society of Chemistry be held responsible for any errors or omissions in this *Accepted Manuscript* or any consequences arising from the use of any information it contains.

ROYAL SOCIETY OF CHEMISTRY

www.rsc.org/materialsC

(revised manuscript ID TC-ART-06-2014-001198 Journal Materials Chemistry C, October 2014)

The role of nanoporosity on local piezo and ferroelectric properties of lead titanate thin films

Alichandra Castro,[a] Paula Ferreira,[a*] Brian J. Rodriguez [b] and Paula M. Vilarinho[a*]

[a] Department of Materials and Ceramics Engineering, Centre for Research in Ceramics and Composite Materials, CICECO, University of Aveiro, Aveiro, Portugal

[b] Conway Institute of Biomolecular and Biomedical Research, University College Dublin, Dublin, Ireland

*corresponding authors (pcferreira@ua.pt, paula.vilarinho@ua.pt)

Journal of Materials Chemistry C Accepted Manuscript

Abstract

Nanoporous and dense ferroelectric $PbTiO_3$ thin films are prepared by a modified sol-gel process. The presence of nanoporosity, with ~ 50 nm pore size formed using a block polymer as a structure-directing agent, markedly affects the microstructure, crystallization and ferroelectric film´s properties. The crystallization of the tetragonal phase is enhanced in nanoporous films. It is suggested that the decomposition of the block-copolymer in porous films triggers the crystallization of the perovskite phase at low temperatures via the local increase of temperature. Consequently, nanoporous films with improved tetragonality exhibit enhanced piezoelectric coefficients, switchable polarization and low local coercivity. By providing a means of achieving enhanced properties, nanoporosity may have a broad impact in applications of ferroelectric thin films.

Keywords

Nanoporosity, ferroelectrics, lead titanate, sol-gel, piezoforce response microscopy

Introduction

Scaling of microelectronics is well known as it responds to the current needs of customers and improves cost, performance, and power of devices.[1] Although it is recognized that, as the transistor size approaches tens of nanometers, the end of planar CMOS transistor scaling is near, there is not yet an alternative. For CMOS technology to react to the challenges of decreasing transistor size,[1] research and development on solutions beyond Moore´s law are indeed required.[2] Scaling traditionally meant reducing feature-size, but currently encompasses wider concepts such as adding functionalities to the device (i.e.,

Journal of Materials Chemistry C Accepted Manuscript

"More than Moore"). This approach does not necessarily meet the scaling requirements of Moore's Law and, as a matter of fact, the functionality may surpass the dimensional aspect.[2]

Within this context, the introduction of porosity at the nanoscale in functional materials (such as ferroelectrics) might be a way, in particular if pores will be functionalized, of creating opportunities to achieve new functionalities and devices. A primary example is a multifunctional composite structure, in which a porous matrix with a narrow pore size distribution is available for further incorporation of a material with a different functional property than the matrix.

The preparation of ordered porous materials started in 1992, when Kresge *et al.*[3] reported that micellar and lyotropic liquid-crystal phases could behave as templates for the formation of mesoporous materials. Initially, mainly silica and aluminosilicate mesoporous with amorphous structures were reported.[4,5] The great attention to mesoporous non-silica oxides started in 1995,[6] when a porous network in TiO_2 powders was first organized. Since then, a large effort has been undertaken to prepare mesoporous non-silica oxide thin films. However, the coexistence of crystallinity and meso-ordering has been shown to be notably difficult.[7] A careful control of chemistry, processing and synthesis treatment conditions are required to avoid the collapse of the meso-ordering during crystallization. In 2004, a controlled process of preparation of ordered mesoporous crystalline networks and mesostructured nano-island single layers, composed of multimetallic oxides having perovskite or ilmenite type structures, was reported.[7] Nanocrystalline mesoporous films of $SrTiO_3$, $MgTa_2O_6$ and $Co_xTi_{(1-x)}O_{(2-x)}$ have been prepared using a copolymer with higher chemical and

Journal of Materials Chemistry C Accepted Manuscript

thermal stability than the often used Pluronics. Cautious control of the self-assembly and kinetics allowed the preservation of the meso-ordering and prevented cation separation during crystallization.

With the purpose of exploring new functionalities of ferroelectrics for micro and nanoelectronics applications, we described the preparation of barium titanate ($BaTiO_3$) and lead titanate ($PbTiO_3$) nanoporous thin films and the piezo and ferroelectric response at the nanoscale of these films in one of our recent works.[8] Although we proved their ferroelectric character, the role of the porosity on the microstructure development and phase evolution and the relations between nanoporosity and the electrical properties at the nanoscale have not been addressed. This is the intent of this work. $PbTiO_3$ with a high polarizibility, strong spontaneous polarization, high Curie temperature (around 490 °C) and high pyroelectric coefficient is the material choice for this study.[9,10] Nanoporous $PbTiO_3$ thin films were prepared through sol–gel templating using a commercial amphiphilic diblock-copolymer, PS40-*b*-PEO53, as a structure-directing agent. The structure and microstructure evolution is followed by X-ray diffraction (XRD), Raman spectroscopy and scanning electron microscopy (SEM). The local electromechanical response is assessed by vertical piezoresponse force microscopy (VPFM) and piezoresponse force spectroscopy (PFS). By comparing the structure and properties of nanoporous and dense $PbTiO_3$ films, prepared under identical conditions, the relations between nanoporosity and local piezoelectric response are established. The role of nanoporosity on the phase and microstructure development of ferroelectric lead titanate films is proposed.

Journal of Materials Chemistry C Accepted Manuscript

Experimental

Porous $PbTiO_3$ films were prepared as described in reference.[8] PS40-b-PEO53 block-copolymer with MWPS = 40 000 $gmol^{-1}$, MWPEO = 53 000 $gmol^{-1}$, from Polymer Source, was used as a structure-directing agent. Three solutions were prepared. In solution A, PS40-b-PEO53 block-copolymer (75 mg, Polymer Source) was dissolved in tetrahydrofuran (5.62 mmol, Sigma-Aldrich, purity ≥ 99.5%) at 70 ºC. Subsequently, and under stirring, absolute ethanol (26.42 mmol, BRAND) was added drop by drop. Solution B was prepared by the dissolution of lead (II) acetate trihydrate (0.60 mmol, Fluka, purity ≥ 99.5% w/w) in glacial acetic acid (Merck) at 70 ºC. Solution C was prepared from mixing 2,4-pentanedione (0.43 mmol, Fluka, purity 99.3% w/w) with titanium (IV) n-butoxide (0.60 mmol, Merck, 98.0% w/w) under stirring at room temperature. Afterwards, solutions B and C were added to solution A, forming the final solution. For the dense thin films, a similar procedure was used, however solution A was prepared without the block-copolymer. Nanoporous and dense thin films were deposited by dip-coating onto platinized silicon ($Pt/TiO_2/SiO_2/Si$) (Inostek Inc.). In order to get similar film thicknesses (around 100 nm), the withdrawal rates were adjusted to 0.493 mm/s (nanoporous) and 0.761 mm/s (dense). All films were thermally treated in air at 350 °C in order to complete the inorganic condensation (mesostructuration) of the matrix and to decompose the organic content. The films were then annealed for 5 min at the desired temperatures to achieve crystallization. To follow the phase formation process, thermal gravimetric and differential thermal analyses (TG-DSC) were carried out on dried nanoporous and dense powders obtained by drying the solutions described above in open vessels at 60 ºC for few days.

Journal of Materials Chemistry C Accepted Manuscript

A Setaram Labsys™ TG-DSC16 system was used with a heating rate of 10 °C/min under flowing air up to 600 °C. The crystalline phases in the films were identified by XRD using a Philips X'Pert MPD X-ray diffractometer with Cu Kα radiation and 2 ° grazing incidence angle. Raman spectroscopy was performed in JY Horiba LabRam model HR800 equipment, with a high resolution 800 mm focal length spectrometer. An argon ion laser beam at a wavelength of 325 nm was utilized. The film mesostructure was investigated by high-resolution SEM using a SU-70 Hitachi microscope. Vertical PFM (VPFM) was carried out on an atomic force microscopy (AFM) system (JPK, Nanowizard II, with a lock in amplifier, SRS Stanford Research Systems), using DPE-18 cantilevers with Pt-coated tips (Mikromasch, resonant frequency of 60−100 kHz, force constant of 1.1−5.6 N/m). Topography signals of the film surface were taken simultaneously with the amplitude and phase signals and were collected in contact mode. Since the results were obtained with the same type of cantilevers and under identical scanning and acquisition conditions, comparison between films can be made. Piezoresponse force spectroscopy (PFS) as function of the applied potential between the platinized substrate and the conducting tips was performed on an MFP-3D AFM (Asylum). Several hysteresis loops with bias from - 8 to + 8 V were obtained for each sample to ensure the reproducibility of the results, and representative loops are presented. The piezoelectric and ferroelectric properties are mean values taken from several hysteresis loops, at least twenty for each sample. The imprint is defined as $I_m = (V^+ + V^-) / 2$, where V^+ correspond to the positive coercive bias and V^- to the negative coercive bias and these bias values were taken from the phase signal. Remanent piezoelectric coefficients were taken from amplitude signal

Journal of Materials Chemistry C Accepted Manuscript

for zero bias values. Switchable polarization corresponds to the difference between the positive saturated piezoresponse and negative ones ($R_m = (R_S)^+ - (R_S)^-$) taken from the mixed hysteresis loops. As the effective piezoelectric coefficient ($(d_{33})_{eff}$) is proportional to the amplitude signal, this can be defined as $(d_{33})_{eff} \propto$ (amplitude signal . cos(phase signal)) / V_{ac}, where V_{ac} is the ac voltage applied. The absolute values of d_{33} were not determined, but as the results were acquired with the same cantilever and under identical scanning and acquisition conditions, the comparison of the relative values of piezoelectric coefficients for each film can be established.

Results and discussion

Figure 1 presents TG-DSC analyses of nanoporous and dense $PbTiO_3$ precursor gels. The TG curves (Figure 1a)) of these gels have a similar profile in which three main regions can be identified: region I from room temperature up to 200 ºC, in which the weight losses for both gels is around 5% and attributed to the loss of residual water and evaporation of organics; region II in which the weight losses are 20% for the case of dense gels (from 200 to 330 ºC) and 32% for the porous ones (from 200 to 450 ºC) and assigned to decomposition of organics; and region III in which the weight losses are almost constant up to 600 ºC, reaching a value of 5% for both gels and attributed to the decomposition of residual species. Note that the temperature interval of region II is wider for nanoporous than for dense precursor gels.

DSC analysis (Figure 1b)) of nanoporous and dense gels also present similar thermal profiles, although the intensity of the thermal effects is different. These curves are characterized by three main thermal effects in the case of

Journal of Materials Chemistry C Accepted Manuscript

nanoporous gels and just two in the case of the dense ones. In the case of nanoporous gels, the two intense exothermic peaks between 200 and ≈450 ºC corresponding to region II in DSC are related with the decomposition of organics and block copolymer degradation. The block copolymer used in the solution preparation is formed by two different copolymers (PS and PEO) with different degradation temperature. The third exothermic one, between 450 and 600 ºC (region III) is attributed to the crystallization of the perovskite phase. In the case of dense gels, just one and less intense peak is observed in the region II. This fact is due to the absence of the block copolymer in this case. The peak observed in the region II corresponds also to the crystallization phase as observed in the nanoporous case. However, in the case of the nanoporous case the crystallization occurs at lower temperature than in the case of the dense. This is in line with the TG behaviour and indicates that the energy released in this temperature interval is higher when compared with dense precursor gels.

Figure 2 depicts top view SEM micrographs of nanoporous and dense $PbTiO_3$ films thermally treated at different temperatures and illustrates the differing microstructure evolution of both films. Nanoporous films thermal treated at 500 ºC (Figure 2), present a porous microstructure with a certain degree of order and periodicity. Pore size is around 50 nm. Pore order and periodicity results from the self-assembly of micelles of the amphiphilic block-copolymer, followed by condensation of the inorganic species around the micelle arrays. During the thermal decomposition of the block-copolymer, void motifs are created. According to the thermal analysis, this takes place between 200 and 400 ºC (Figure 1). As the temperature of the heat treatment increases, the microstructure of the porous films varies, from a somehow organized pore

Journal of Materials Chemistry C Accepted Manuscript

arrangement to an interconnected porosity. At 550 ºC, the walls between the pores start to collapse and pores become connected, but the film remains porous. For high temperature treatments, pore connectivity increases and simultaneously the relative area of dense zones increases as well, corresponding to film densification promoted by the heat treatment. For films treated at 600 and 625 ºC, the organization of the pores is significantly degraded. In addition, as the treatment temperature increases, bright areas appear (~ 550 ºC), which become increasingly larger. Comparatively and as expected, the microstructure is dense and crack-free for the case of dense films. These films heat treated at 550 ºC are amorphous. As the annealing temperature increases, dense films crystallize and a well-defined grain pattern can be observed. The growth of the grains is evident in films annealed at 625 ºC.

Figure 3 shows the XRD patterns of nanoporous and dense $PbTiO_3$ films treated at different temperatures. Nanoporous films heat treated at 550 ºC are mainly amorphous but some diffraction peaks associated with crystalline $PbTiO_3$ are already visible at *ca*. 22, 32 and 45º 2θ. At this temperature, it is not possible to differentiate between the cubic and tetragonal structure of $PbTiO_3$ (JCPDS no. 00-040-0099 and 00-003-0721, respectively). For heat treatments at and above 575 ºC, the film crystallinity increases and the tetragonal phase can be easily identified by the splitting of the diffraction peaks at 22.43, 31.92 and 45.79 into 21.45, 22.78, 31.47, 32.77, 43.69 and 47.56 º 2θ, respectively. However, the concomitant presence of both cubic and tetragonal phases is possible. In the case of the dense films, those heat treated at 550 ºC are clearly amorphous (Figure 3). At 575 ºC, dense films start to show some degree of crystallinity. The tetragonal crystallographic phase is visible for the heat

Journal of Materials Chemistry C Accepted Manuscript

treatment of 625 ºC, with a clear splitting of the diffraction peaks as described above. These results confirm the previous indications that $PbTiO_3$ nanoporous films crystalize at lower temperatures than their dense counterparts.

To verify these observations, Raman spectroscopy studies were conducted (Figure 4). Nanoporous films treated at 525 ºC do not present the typical Raman modes of the tetragonal phase. However, for films heat treated at 575 ºC or 625 ºC, the presence of E+B1, A1 (2TO), E(3TO) and A1(3TO) bands at 287, 324, 503 and 599 cm^{-1}, respectively, indicate the presence of the tetragonal phase, as previously reported for other $PbTiO_3$ and lead zirconate titanate thin films.[11-13] The Raman peaks are slightly shifted to low wavenumber in relation to single crystal values,[14] probably due to strains induced by the substrate. In the case of dense thin films, tetragonal modes start to be observed only at 625 ºC, in agreement with the XRD observations. The formation of the tetragonal phase in nanoporous $PbTiO_3$ films occurs at a lower temperature than in the case of dense ones. Because the tetragonal phase is the one responsible for ferroelectricity in ABO_3 perovskite type materials, we therefore expect some differences in terms of the electrical/electromechanical behaviour between these films.

The local piezoelectric and ferroelectric behaviour of nanoporous and dense films were investigated through vertical piezoresponse force microscopy (VPFM) and piezoresponse force spectroscopy (PFS). Figures 5 and 6 represent the topography and VPFM amplitude and phase images of nanoporous and dense $PbTiO_3$ films thermally treated at different temperatures. The dark domains in the VPFM phase images correspond to domains in which the polarization is oriented towards the substrate (phase = -180 °), while bright

Journal of Materials Chemistry C Accepted Manuscript

regions correspond to domains with polarization oriented towards the free surface of the films (phase = 180 °). Since sol-gel and self assembly methods have as a drawback a random size distribution of the deposited nanograins and, VPFM is sensitive to the component of polarization normal to the film surface, grains with in-plane polarization exhibit an intermediate contrast. Nanoporous films thermally treated at 500 and 525 ºC do not present piezoelectric response what is related with their incipient degree of crystallinity. In the topography images of the different nanoporous films, pores and grains are not clearly defined due to the use of contact mode, in which the tip convolution effect is more evident.[8] For all nanoporous films, the topography and VPFM amplitude and phase images reveal the presence of two distinct phases exhibiting different piezoelectric behaviour, in analogy with the two regions (bright and dark) observed in the SEM microstructures (Figure 2). The dimension of the area with strong piezoelectric response (the bright areas in SEM micrographs) increases with the increase of the heating temperature, and in accordance with the enhancement of the degree of crystallinity and tetragonal distortion as observed by XRD and Raman (Figure 3 and 4).The bright areas formation can be related with a kinetic process of nucleation and as these bright areas are more defined in the nanoporous films than in dense ones, the pores in the nanoporous case probably act as nucleation defects contributing for a early crystallization. This is well known from the nucleation and crystal growth classic theories.[15] However, experimentally, it was difficult to maximize the areas with strong piezoelectric behaviour without losing the porosity order.

VPFM amplitude and phase images of dense films (Figure 6) show that the piezoelectric domains in these films are smaller and less defined than in the

Journal of Materials Chemistry C Accepted Manuscript

case of nanoporous ones. Moreover, aaccording to the domain size analysis, Table 1, the piezoelectric domains in dense films are smaller than in the case of nanoporous ones. This fact is a consequence of high crystallinity present in the nanoporous films. However, as the annealing temperature increases in the case of nanoporous films, the domains size decreases showing the grains of these films are polydomains as consequence of the grain size and the methodology used to prepare the thin films. At 550 ºC, no VPFM response could be observed in dense films, corroborating the observations of XRD and Raman spectroscopy. VPFM response is only observed for films heat treated at temperatures above 575 ºC. An increase of the area exhibiting VPFM response is also observed with enhanced annealing temperature.

The representative PFS results obtained from the bright areas of these films are shown in Figure 7. The representative remanent hysteresis loops (amplitude and phase) reveal that the switched polarization remains after bias removal. For each film, hysteresis loops were measured from individual domains. The well-defined hysteresis loops clearly confirm the ferroelectric behaviour at room temperature of nanoporous and dense $PbTiO_3$ films heat treated at different temperatures: 550, 600 and 625 ºC in the case of nanoporous and 575, 600 and 625 ºC for dense ones. However, the obtained phase hysteresis loops are not symmetric in terms of coercive voltage and remanent polarization for all films. This effect is known as imprint and is usually caused by the preference of a certain polarization state over the other. Thus, the horizontal shift present in all the hysteresis loops provides a measure of the internal field, and the vertical shift present in the same hysteresis loops provides information on regions with frozen polarization, i.e., can be associated with regions having a non-switching

Journal of Materials Chemistry C Accepted Manuscript

or preferentially oriented polarization.[16] Imprint behaviour can also be related to the self-polarization that depends, to a large extent, on the film deposition technology. The phenomenon of self-polarization occurs due to the presence of an internal electric field, which is at least as large as the coercive field at the Curie temperature. In the case of sol–gel deposited films, it was reported that the self-polarization effect is thickness dependent, suggesting that the alignment of domains occurs locally near the film–bottom electrode interface.[17-19] As in our work, the thickness is practically the same for nanoporous and dense films (around 100 nm), the vertical shift is not evaluated. Table 2 presents mean values of imprint, critical voltage, coercivity, and remanent piezoelectric coefficients calculated from several phase and amplitude hysteresis loops measured for nanoporous and dense films. Table 2 presents also the switchable polarization and $(d_{33})_{eff}$, calculated from mixed hysteresis loops. From the imprint values, the imprint effect can be associated with an incipient crystallization of the tetragonal phase. Thus, as the heating temperature increases, imprint is slightly decreased (Table 2). Another explanation for this imprint effect is the presence of defects in the film, including oxygen vacancies and surface/interface defects (lattice distortion due to the difference of the thermal expansion coefficient between the film and the substrate). From critical voltage and coercivity values of Table 2, it is observed that nanoporous films present values slightly lower when compared with the dense thin films, suggesting that the crystallinity degree and porosity present in nanoporous films can affect the switching ability. Thus, and whereas the critical voltage values are usually used to evaluate the switching capability, the nanoporous films show a higher switching ability than the dense films.

Journal of Materials Chemistry C Accepted Manuscript

The switching process starts with the nucleation of a new domain just under the tip. This newly formed domain expands until it reaches an equilibrium size, which depends on the value of applied voltage. This nucleation and growth of reverse domains are responsible for the reverse polarization. As discussed previously, the porosity in the films triggers the crystallization at lower temperature than in dense counterparts. Thus, we propose that this earlier crystallization of the tetragonal perovskite phase (prompted by the presence of porosity) leads to a reduction of the energy necessary to reorient the dipoles in the ferroelectric structures and, consequently a reduction of coercivity when compared with dense films. On the other hand, as the porosity induces instability in the dipole-dipole interactions, the reverse polarization can be favoured for low bias values, Table 2.

Thus, in this work we show that both the presence and increasing of porosity content decreases the effective coercive field in nanoporous films. Remanent piezoelectric coefficients, $(d_{33})_{eff}$ coefficients and switchable polarization are higher for nanoporous than for dense films, revealing that porosity leads to better ferroelectric properties. This can be also related to the crystallinity of the films, probably to the high content of tetragonal phase present in the nanoporous films and associated with a smaller constraining effect of the substrate as well, when compared with equivalent dense films. Porosity is known to decrease the polarization and the dielectric permittivity of a polar media. Though deleterious, the decrease of permittivity can be beneficial to the pyroelectric coefficients of a ferroelectric material, as previously observed in several perovskites, like lead calcium titanate porous films.[20] However, the

Journal of Materials Chemistry C Accepted Manuscript

effect of porosity on the intrinsic behaviour of switching of a ferroelectric has never been reported before.

The increase of the piezoelectric coefficient and decrease of the coercive field for nanoporous films as observed and reported for the first time in this work are very important results, since they can be used as a tool to tailor the coercive field of ferroelectric nanostructures. Thus, nanoporosity can be viewed as a strategy to respond to the current miniaturization requirements of microelectronics; a good example is the application of these structures in ferroelectric capacitors for non-volatile ferroelectric random access memories (FeRAMs) in which the switchable remanent polarization should be reversed by application of short bias voltage.[21] However further studies are required ideally supported by modelling the effect of nanoporosity on the local electric field of porous and dense films.

Conclusions

Nanoporous and dense PbTiO3 thin films were prepared by a modified sol-gel route. The porosity structure and arrangement is very dependent on the heat treatment; as the temperature of annealing increases, the porosity tends to collapse and films tend to densify. An earlier crystallization of the tetragonal perovskite phase was verified to occur in nanoporous films when compared with the dense counterparts. A possible explanation for the observed effect can be related with the exothermic degradation of block copolymer (strengthened by the intense peaks observed in the DSC) concomitant with the presence of the pores that act as nucleation defects contributing for the formation of tetragonal phase at lower temperature in nanoporous films than in dense ones.[15] This enhancement of the

Journal of Materials Chemistry C Accepted Manuscript

tetragonality of the nanoporous films is reflected in the enhancement of the local ferroelectric properties. Under the same processing conditions, porous films show a higher local piezoelectric response and, importantly a lower local coercive field than the dense counterpart. Though further studies are required, nanoporosity might be a tool to improve the switching behaviour of ferroelectric thin films.

Acknowledgements

Authors are grateful to FCT, FEDER, QREN-COMPETE for funding the project FCOMP-01-0124-FEDER-009356 (PTDC/CTM/098130/2008), Associate Laboratory CICECO FCOMP-01-0124-FEDER-037271 (Pest-C/CTM/LA0011/2013) and Doctoral fellowship SFRH/BD/67121/2009. P. Ferreira acknowledges FCT for IF/00327/2013. Some of the measurements were performed on equipment funded by Science Foundation Ireland (SFI07/IN1/B931). We acknowledge COST Action MP0904 SIMUFER for funding the Short Term Scientific Mission of A. Castro. We acknowledge Denise Denning from the Nanoscale Function group of Conway Institute of Biomolecular and Biomedical Research for assistance and discussion related with the Scanning Probe Microscopy measurements.

References

1. S. E. Thompson and S. Parthasarathy, *Materials Today*, 2006, **9**, 20;
2. http://www.itrs.net;
3. C. T. Kresge, M. E. Leonowicz, w. J. Roth, J. C. Vartuli and J. S. Beck, *Nature*, 1992, **359**, 710;
4. C. Sanchez, C. Boissière, D. Grosso, C. Laberty, and L. Nicole, *Chemistry of Materials*, 2008, **20**, 682;.
5. G. J. D. A. A. Soler-Illia, C. Sanchez, B. Lebeau, and J. Patarin, *Chemical reviews*, 2002, **102**, 4093;

Journal of Materials Chemistry C Accepted Manuscript

6. D. M. Antonelli and J. Y. Ying, *Angewandte Chemie International Edition English*, 1995**, 34,** 2014;

7. D. Grosso, C. Boissière, B. Smarsly, T. Brezesinski, N. Pinna, P. a Albouy, H. Amenitsch, M. Antonietti, and C. Sanchez, *Nature materials*, 2004, **3**, 787;

8. P. Ferreira, R. Z. Hou, A. Wu, M.-G. Willinger, P. M. Vilarinho, J. Mosa, C. Laberty-Robert, C. Boissière, D. Grosso, and C. Sanchez, *Langmuir : the ACS journal of surfaces and colloids*, 2012, **28**, 2944;

9. J. Harjuoja, A. Kosola, M. Putkonen, and L. Niinistö, *Thin Solid Films*, 2006, **496**, 346;

10. D. G. Wang, C. Z. Chen, J. Ma, and T. H. Liu, *Applied Surface Science*, 2008, **255**, 1637;

11. I. Taguchi, a. Pignolet, L. Wang, M. Proctor, F. Lévy, and P. E. Schmid, *Journal of Applied Physics*, 1993, **74**, 6625;

12. I. Taguchi, a. Pignolet, L. Wang, M. Proctor, F. Lévy, and P. E. Schmid, *Journal of Applied Physics*, 1993, **73**, 394;

13. Z. C. Feng, B. S. Kwak, a. Erbil, and L. a. Boatner, *Applied Physics Letters*, 1994, **64**, 2350;

14. R. A. Frey and E. Silberman, *Helvetica Physica Acta*, 1976, **49**, 1;

15. C. Barry Carter and M. Grant Norton, Ceramic Materials, Science and Engineering, Springer Science, New York, 2nd edition, 2007, chapter 24, pp. 427-441;

16. M. Alexe, C. Harnagea, D. Hesse, and U. Gösele, 2001, **79**, 242;

17. A. L. Kholkin, K. G. Brooks, D. V. Taylor, S. Hiboux, and N. Setter, *Integrated Ferroelectrics*, 1998, **22**, 525;

18. J. Frey, F. Schlenkrich, and A. Schönecker, *Integrated Ferroelectrics*, 2001, **35**, 105;

19. A. Wu, P. M. Vilarinho, V. V Shvartsman, G. Suchaneck, and A. L. Kholkin, *Nanotechnology*, 2005, **16**, 2587;

20. A. Seifert, *Journal of Sol-Gel Science and Technology,* 1999, **20**, 13;

21. J. Li, B. Nagaraj, H. Liang, W. Cao, C. H. Lee, and R. Ramesh, *Applied Physics Letters*, 2004, **84**, 1174.

Journal of Materials Chemistry C Accepted Manuscript

Figure and Tables Captions

Figure 1: TG-DSC of precursor gels of nanoporous and dense $PbTiO_3$ films. The TG curves of nanoporous and dense gels are quite very similar, with a significant weight loss from room temperature up to 450 ºC. The DSC curves clearly show that the crystallization occurs at an earlier temperature in the case of the nanoporous films when compared with the dense ones.

Figure 2: SEM micrographs illustrating the typical morphology of nanoporous and dense $PbTiO_3$ films after thermal treatment at: 500, 550, 575, 600 and 625 ºC. As the temperature of the thermal treatment increases, the porosity order is lost, pores become interconnected and dense areas increase. A well-defined grain pattern with increasing of grain size with annealing temperature characterizes $PbTiO_3$ dense films.

Figure 3: X-ray diffraction patterns of nanoporous and dense $PbTiO_3$ films thermally treated at: 500, 550, 575, 600 and 625 ºC. Solid black vertical lines correspond to the tetragonal (JCPDS no 00-003-0721) and dashed vertical lines correspond to cubic (JCPDS no 00-040-0099) crystalline phase of $PbTiO_3$. The gray lines correspond to the Pt layer of the substrate. Tetragonal $PbTiO_3$ phase crystallizes at lower temperatures in the case of nanoporous films (575 ºC).

Figure 4: Raman spectra of nanoporous and dense $PbTiO_3$ films thermally treated at: 500, 550, 575, 600 and 625 ºC. Raman spectroscopy proves the early crystallization of tetragonal $PbTiO_3$ phase in nanoporous films.

Journal of Materials Chemistry C Accepted Manuscript

Figure 5: Topographic and VPFM amplitude and phase images of nanoporous $PbTiO_3$ films after thermal treatment at 550, 575, 600 and 625 ºC. The data scale for all topographic images is between 0 to 25 nm, for amplitude at 575, 600 and 625 ºC is between 0 to 250 pm and for all phase images is between -10 to 10 V. This 20 V scale corresponds to 360 º, thus opposite domains oscillate 180 º out of phase, as expected. The dimension of the areas with strong piezoelectric behaviour increases as the heating temperature increases as a consequence of the increasing crystallinity and tetragonal phase content.

Figure 6: Topographic and VPFM phase and amplitude images of dense $PbTiO_3$ films after thermal treatment at: 550, 575, 600, and 625 ºC. The data scale for all topographic images is between 0 to 10 nm, for amplitude at 575, 600 and 625ºC is between 0 to 60 pm and for all phase images is between -10 to 10 V. This 20 V scale corresponds to 360 º, thus opposite domains oscillate 180 º out of phase, as expected. Piezoelectric domains in these films are smaller and less defined than in porous films. In this case, PFM amplitude response appears in films treated at higher heating temperatures when compared with nanoporous ones.

Figure 7: Representative remanent local hysteresis loops: phase (a and c) and amplitude (b and d) obtained in nanoporous and dense $PbTiO_3$ films after thermal treatment at: 550, 575, 600 and 625 ºC. Ferroelectric properties are enhanced in nanoporous films.

Table 1: Domain size for nanoporous and dense thin films calculated from the amplitude image.

Journal of Materials Chemistry C Accepted Manuscript

Table 2: Average values of critical voltage, coercivity, imprint, switchable polarization, remanent piezoelectric coefficients and $(d_{33})_{eff}$ calculated from several phase, amplitude and mixed hysteresis loops for all nanoporous and dense thin films. The lower coercivity values present in nanoporous films show that the nanoporosity favours the switching in this kind of structure.

Journal of Materials Chemistry C Accepted Manuscript

Figures and tables

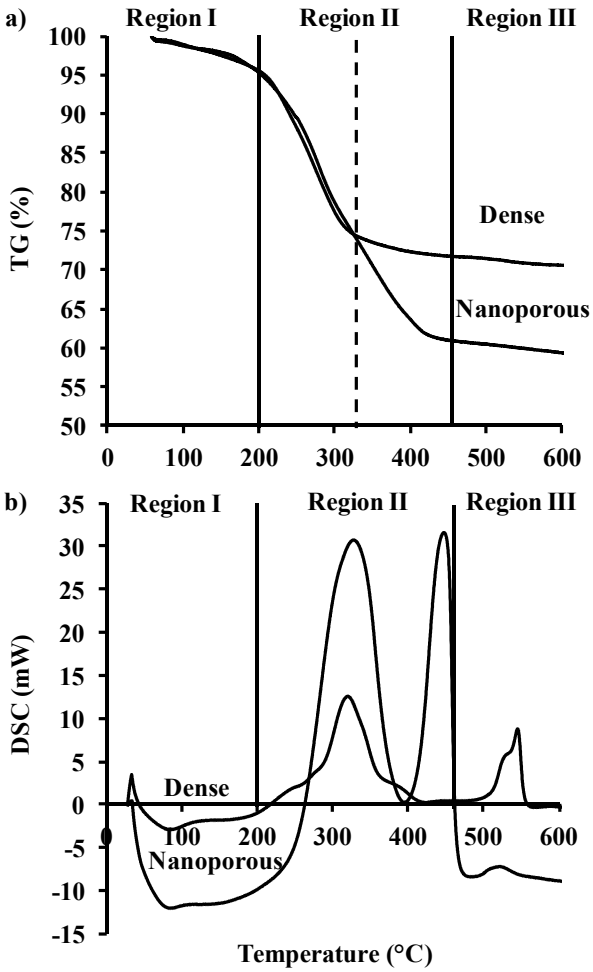

Figure 1: TG-DSC of precursor gels of nanoporous and dense $PbTiO_3$ films. The TG curves of nanoporous and dense gels are quite very similar, with a significant weight loss from room temperature up to 450 ºC. The DSC curves clearly show that the crystallization occurs at an earlier temperature in the case of the nanoporous films when compared with the dense ones.

Journal of Materials Chemistry C Accepted Manuscript

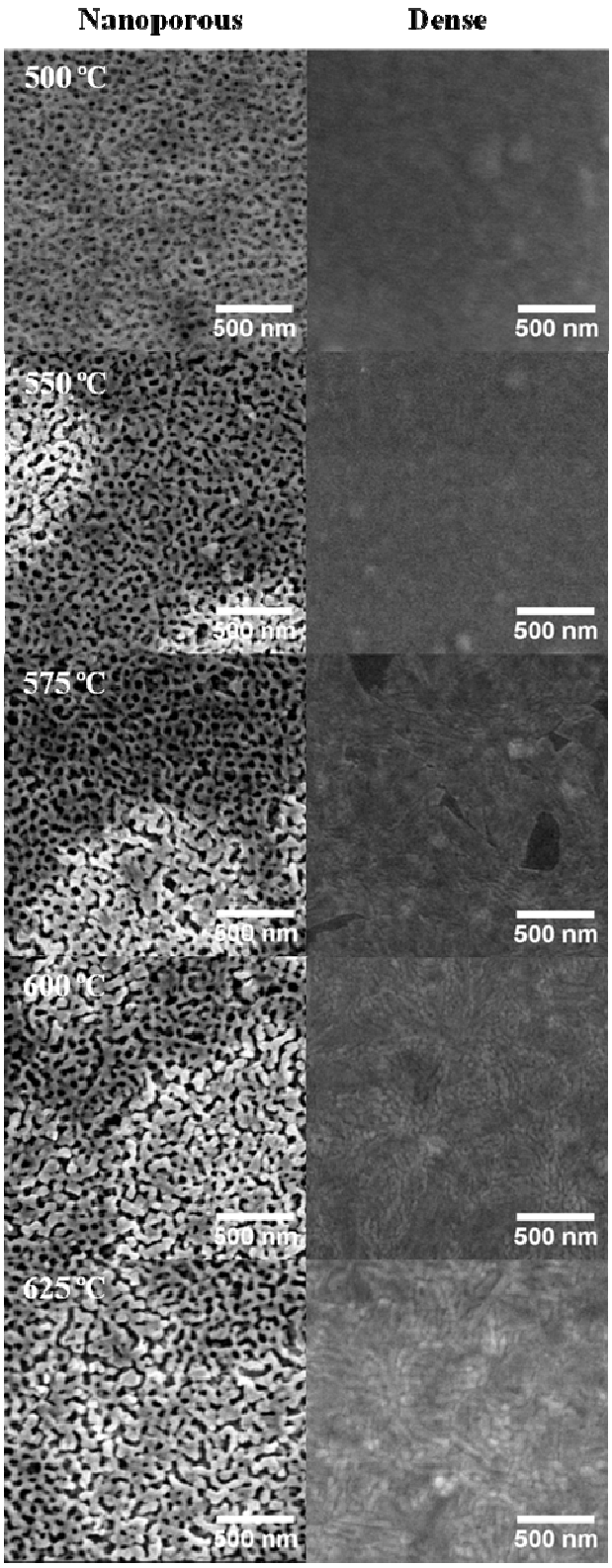

Figure 2: SEM micrographs illustrating the typical morphology of nanoporous and dense $PbTiO_3$ films after thermal treatment at: 500, 550, 575, 600 and 625 ºC. As the temperature of the thermal treatment

Journal of Materials Chemistry C Accepted Manuscript

increases, the porosity order is lost, pores become interconnected and dense areas increase. A well-defined grain pattern with increasing of grain size with annealing temperature characterizes $PbTiO_3$ dense films.

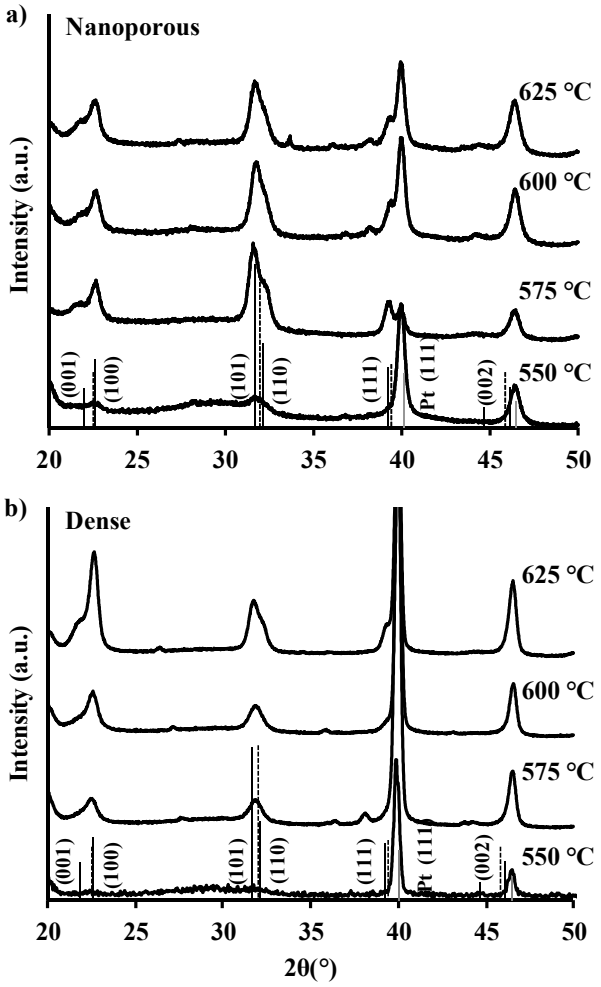

Figure 3: X-ray diffraction patterns of nanoporous and dense $PbTiO_3$ films thermally treated at: 500, 550, 575, 600 and 625 ºC. Solid black vertical lines correspond to the tetragonal (JCPDS no 00-003-0721) and dashed vertical lines correspond to cubic (JCPDS no 00-040-0099) crystalline phase of $PbTiO_3$. The gray lines correspond to the Pt layer of the substrate. Tetragonal $PbTiO_3$ phase crystallizes at lower temperatures in the case of nanoporous films (575 ºC).

Journal of Materials Chemistry C Accepted Manuscript

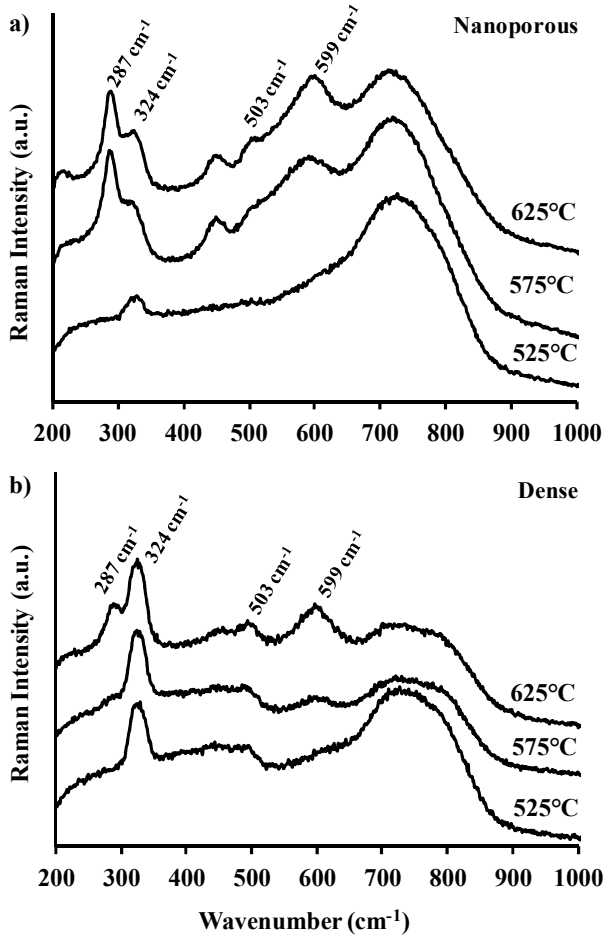

Figure 4: Raman spectra of nanoporous and dense $PbTiO_3$ films thermally treated at: 500, 550, 575, 600 and 625 ºC. Raman spectroscopy proves the early crystallization of tetragonal $PbTiO_3$ phase in nanoporous films.

Journal of Materials Chemistry C Accepted Manuscript

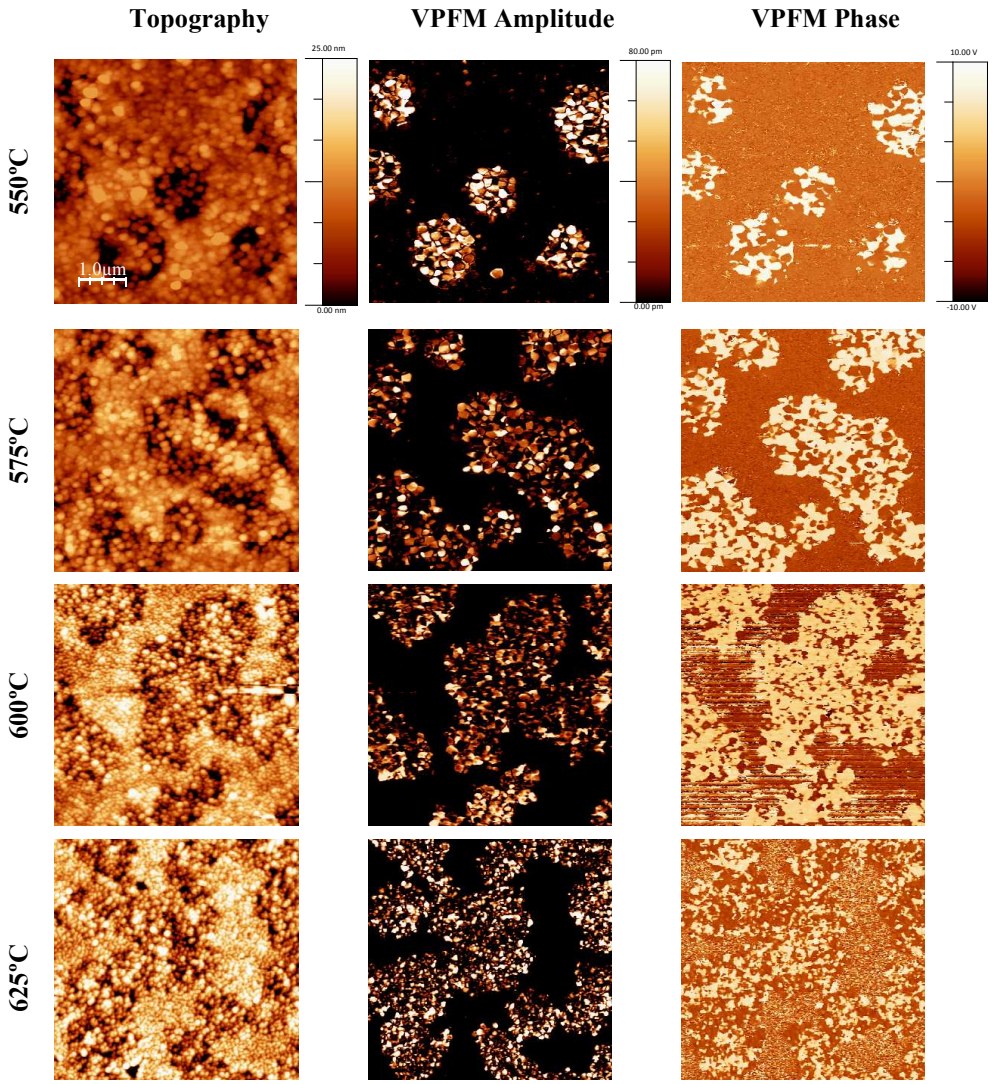

Figure 5: Topographic and VPFM amplitude and phase images of nanoporous $PbTiO_3$ films after thermal treatment at 550, 575, 600 and 625 ºC. The data scale for all topographic images is between 0 to 25 nm, for amplitude at 575, 600 and 625 ºC is between 0 to 250 pm and for all phase images is between -10 to 10 V. This 20 V scale corresponds to 360 º, thus opposite domains oscillate 180 º out of phase, as expected. The dimension of the areas with strong piezoelectric behaviour increases as the heating temperature increases as a consequence of the increasing crystallinity and tetragonal phase content.

Journal of Materials Chemistry C Accepted Manuscript

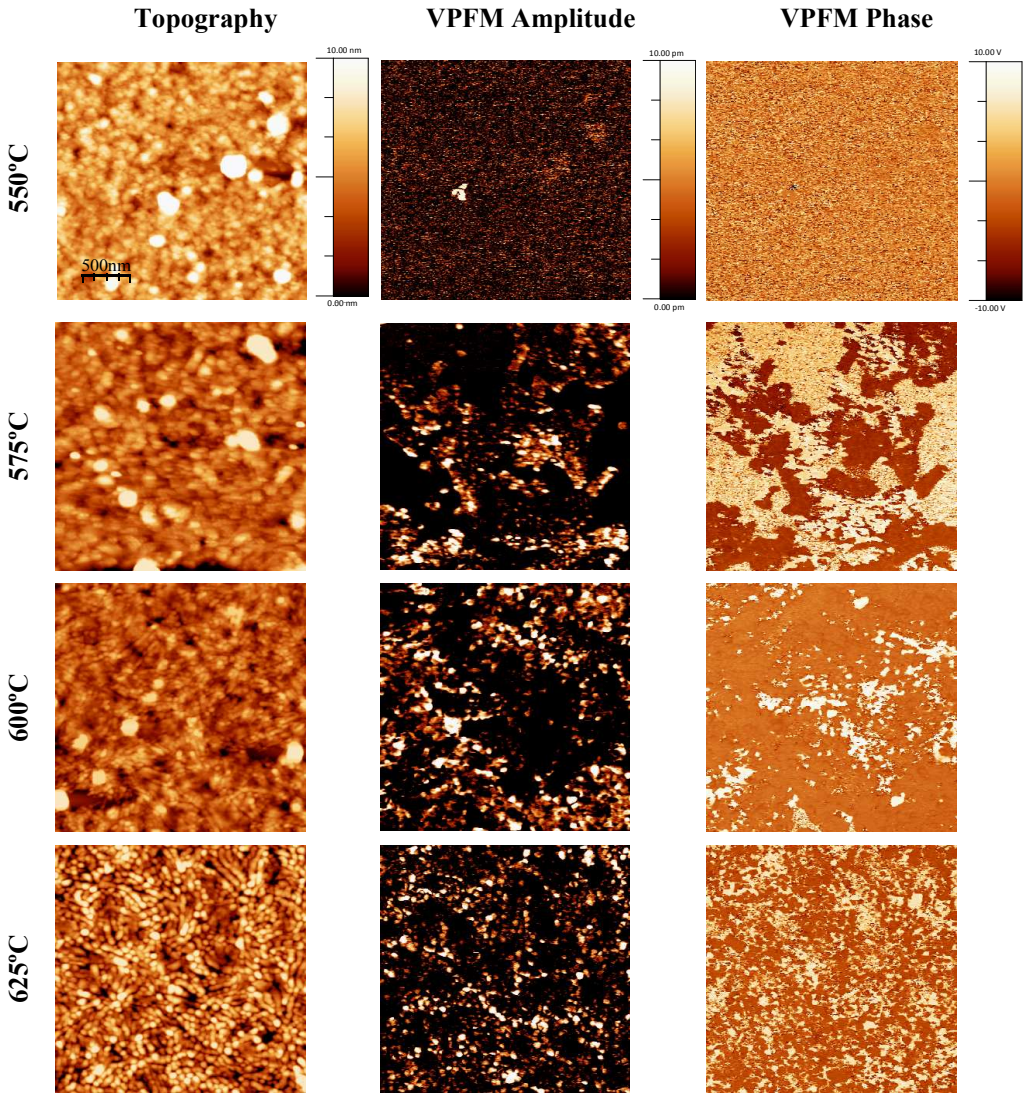

Figure 6: Topographic and VPFM phase and amplitude images of dense $PbTiO_3$ films after thermal treatment at: 550, 575, 600, and 625 ºC. The data scale for all topographic images is between 0 to 10 nm, for amplitude at 575, 600 and 625ºC is between 0 to 60 pm and for all phase images is between -10 to 10 V. This 20 V scale corresponds to 360 º, thus opposite domains oscillate 180 º out of phase, as expected. Piezoelectric domains in these films are smaller and less defined than in porous films. In this case, PFM amplitude response appears in films treated at higher heating temperatures when compared with nanoporous ones.

Journal of Materials Chemistry C Accepted Manuscript

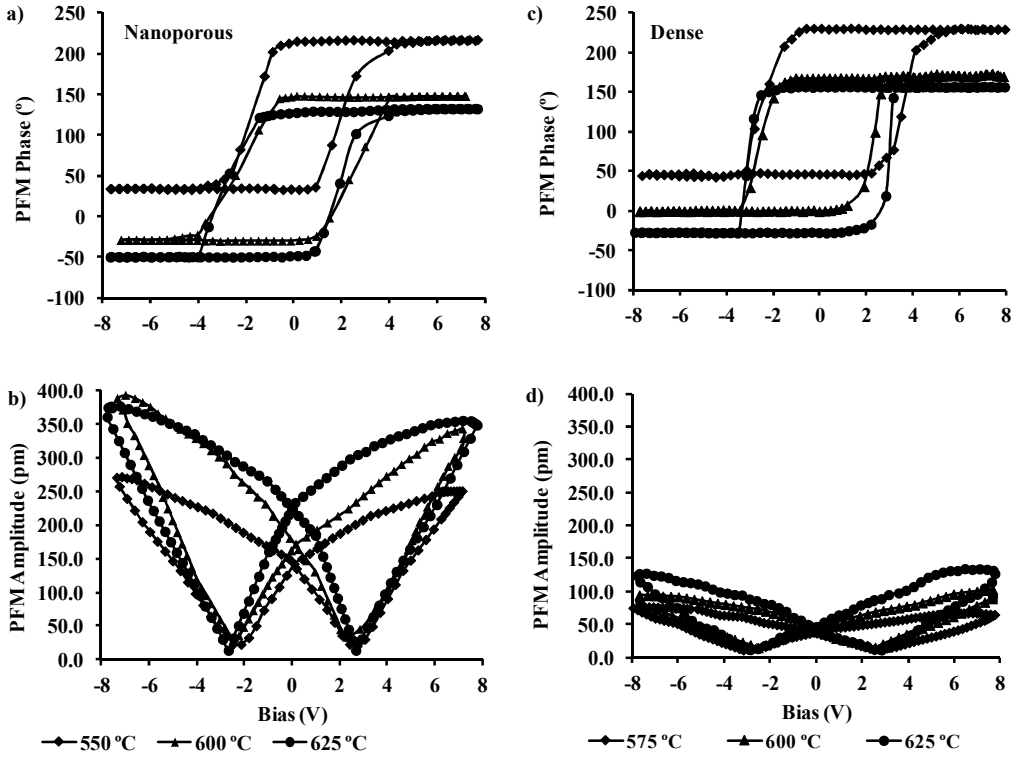

Figure 7: Representative remanent local hysteresis loops: phase (a and c) and amplitude (b and d) obtained in nanoporous and dense $PbTiO_3$ films after thermal treatment at: 550, 575, 600 and 625 ºC. Ferroelectric properties are enhanced in nanoporous films.

Journal of Materials Chemistry C Accepted Manuscript

Table 1: Domain size for nanoporous and dense thin films calculated from the amplitude image.

Heating temperature (º C)	Nanoporous (nm)	Dense (nm)
550	210.8 ± 15.9	
575	206.4 ± 16.9	49.3 ± 7.9
600	196.2 ± 14.6	49.8 ± 6.9
625	119.2 ± 14.1	51.5 ± 8.3

Table 2: Average values of critical voltage, coercivity, imprint, switchable polarization, remanent piezoelectric coefficients and $(d_{33})_{eff}$ calculated from several phase, amplitude and mixed hysteresis loops for all nanoporous and dense thin films. The lower coercivity values present in nanoporous films show that the nanoporosity favours the switching in this kind of structure.

	Heating temperature (º C)	Critical voltage (V)	Coercivity values (V)	Imprint values (V)	Switchable polarization (pm/V)	Remanent piezoelectric coefficient (pm)	$(d_{33})_{eff}$ (pm/V))
Nanoporous films	**550**	1.0±0.1	2.0±0.1	0.9±0.1	254.7±6.8	149.1±5.3	137.0±5.7
	600	1.0±0.1	2.4±0.1	1.0±0.1	261.3±6.6	172.4±5.8	148.8±5.5
	625	1.4±0.1	2.3±0.1	0.5±0.1	534.7±8.3	241.9±6.0	218.8±6.3
Dense films	**575**	2.1±0.1	3.1±0.1	1.1±0.1	65.0±2.9	40.7±0.6	33.4±0.9
	600	1.8±0.1	2.5±0.1	1.2±0.1	85.1±2.0	45.5±0.5	35.7±0.8
	625	2.4±0.1	2.9±0.1	0.8±0.1	107.7±1.3	44.4±1.3	37.8±0.6

Journal of Materials Chemistry C Accepted Manuscript

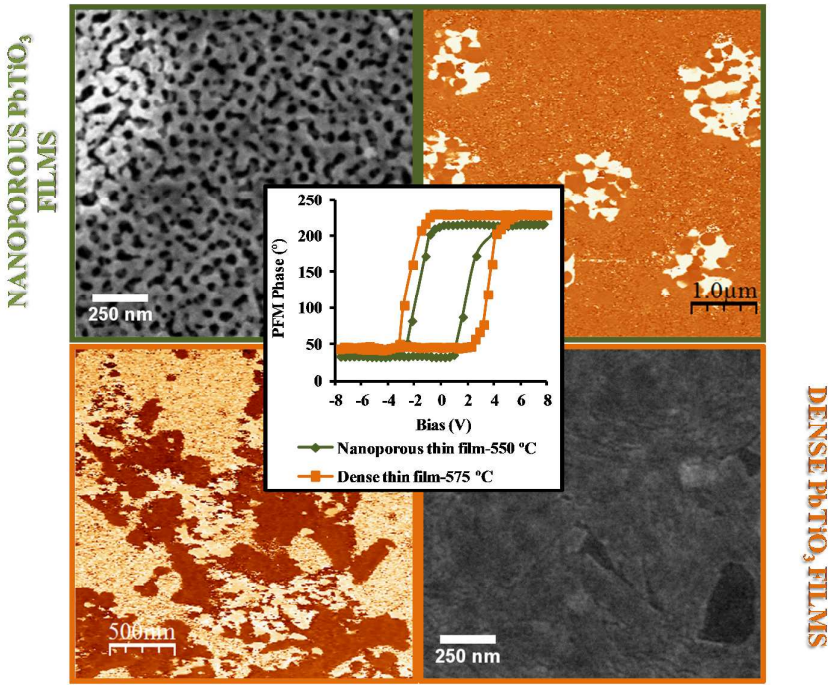

Nanoporous $PbTiO_3$ films present enhanced tetragonality at lower temperature than respective dense films. Moreover, the porosity present in the nanoporous films allows an increase of the local piezoelectric response and a decrease of the local coercive field. As result, these nanoporous films might be used to improve switching behaviour of ferroelectric thin films

Journal of Materials Chemistry C Accepted Manuscript